Title
APPARENT HORIZONTAL SOURCE POSITIONS AND EXIT DIRECTIONS FOR NEGATIVE SECONDARY BEAMS FROM THE BEVATRON

Author
Goorjian, Peter M.

Publication Date
1963-03-19

UCRL-10705

University of California

Ernest O. Lawrence Radiation Laboratory

APPARENT HORIZONTAL SOURCE POSITIONS AND EXIT DIRECTIONS FOR NEGATIVE SECONDARY BEAMS FROM THE BEVATRON

Berkeley, California

DISCLAIMER

Printed in USA. Price 50 cents. Available from the
Office of Technical Services
U. S. Department of Commerce
Washington 25, D.C.

APPARENT HORIZONTAL SOURCE POSITIONS AND EXIT DIRECTIONS FOR NEGATIVE SECONDARY BEAMS FROM THE BEVATRON

Peter M. Goorjian

Lawrence Radiation Laboratory
University of California
Berkeley, California

March 19, 1963

ABSTRACT

An explanation is presented for using the three "Source Maps" referring respectively to current markers 26, 29, and 33. These maps determine the apparent horizontal source position and exit path for any beams travelling in the median plane, which can emerge from an internal Bevatron target with a zero degree production angle. This information can be obtained in a few seconds using a straightedge. The method of map construction is described, and the probable uncertainty in source location is discussed. The various target magnifications are presented.

APPARENT HORIZONTAL SOURCE POSITIONS AND EXIT DIRECTIONS FOR NEGATIVE SECONDARY BEAMS FROM THE BEVATRON

Peter M. Goorjian

Lawrence Radiation Laboratory
University of California
Berkeley, California

March 19, 1963

INTRODUCTION

I. USE OF SOURCE MAPS

Each map shows a polar coordinate plot of the Quadrant II (west) and Quadrant III (north) experimental areas. Reduced prints of drawings 13L1945, 13L1955, and 13L1965A are shown as Figs. 1, 2, and 3, respectively. An angle θ is measured in milliradians from the Gauge Line at the end of the quadrant, and the radial coordinate numbers give $\rho = (r - R_0)$ in inches, where $R_0 = 599\text{-}3/8$ in. = nominal beam center line. Two sets of contour lines are shown, the upper set labeled Source Position Contours, and the lower Direction Contours. The sign of θ is positive as the point is downstream from the gauge line, and negative as the point is upstream.

A. Applications

The following applications demonstrate uses of the source maps:

(a) Given a target location (R_0, θ_t), to determine the apparent horizontal source for a chosen momentum (p BeV/c) beam.

This is given directly by the Source Position Contours as the intersection of the θ_t contour with the appropriate momentum (p) contour.

Example: p = 0.7 BeV/c;

Target coordinates: $\rho = 0$ in., $\theta_t = -105$ mrad (at CM 26);

Source coordinates: $\rho_s = -26$ in., $\theta_s = -83$ mrad;

(b) Given a target location (R_0, θ_t), to determine the line of flight of the beam (momentum = p BeV/c) emerging from the Bevatron.

Determine the apparent source (ρ_s, θ_s) as described in (a).

Next, enter the lower Direction Contour plot along the lines θ_t and p and find their intersection (ρ_D, θ_D). The straight line joining (ρ_s, θ_s) and

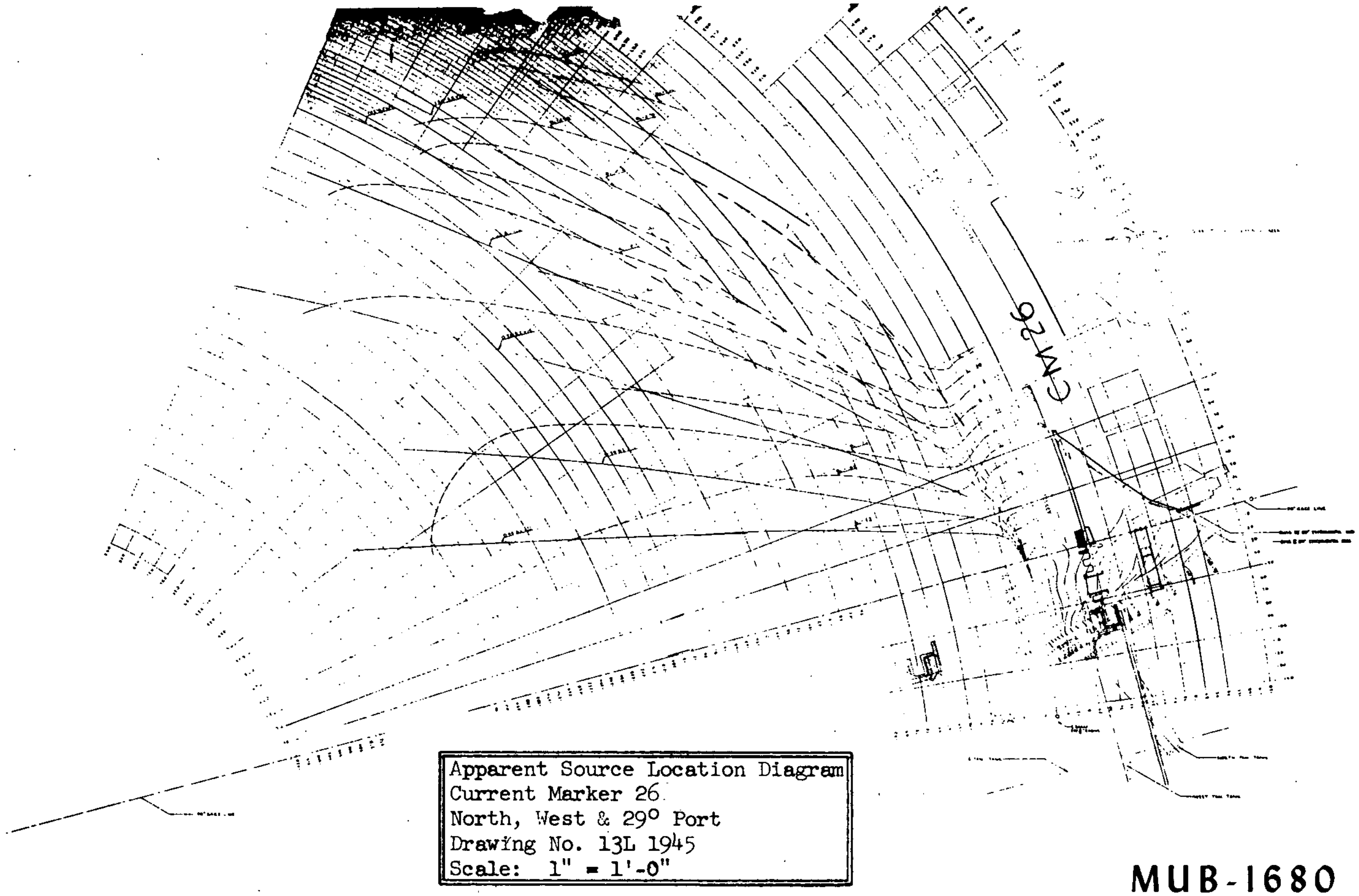

Fig. 1. Reduced version of Bevatron map showing Source Point and Direction Contours at CM 26 (Dwg. No. 13L1945).

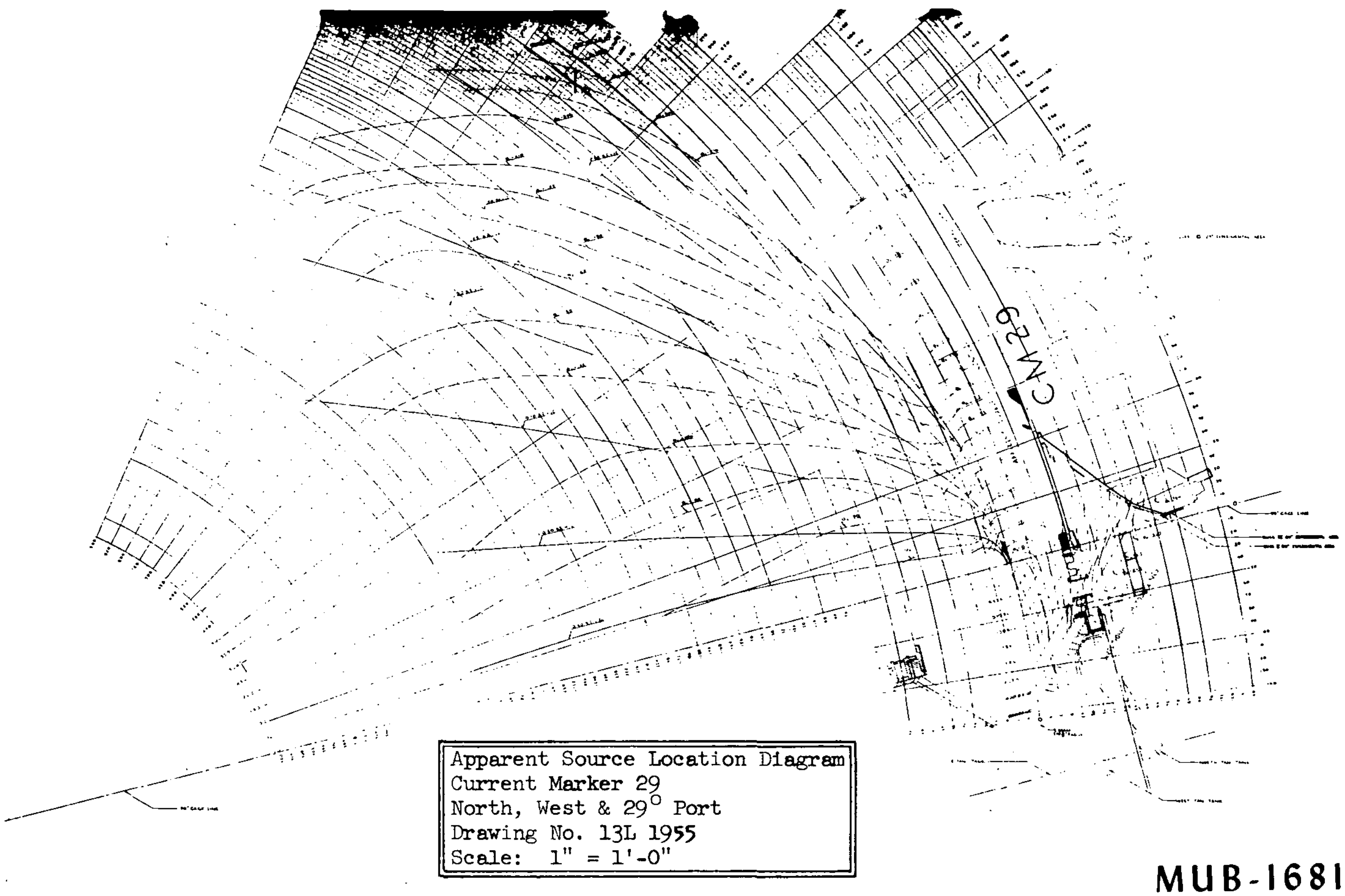

Fig. 2. Reduced version of Bevatron map showing Source Point and Direction Contours at CM 29 (Dwg. No. 13L1955).

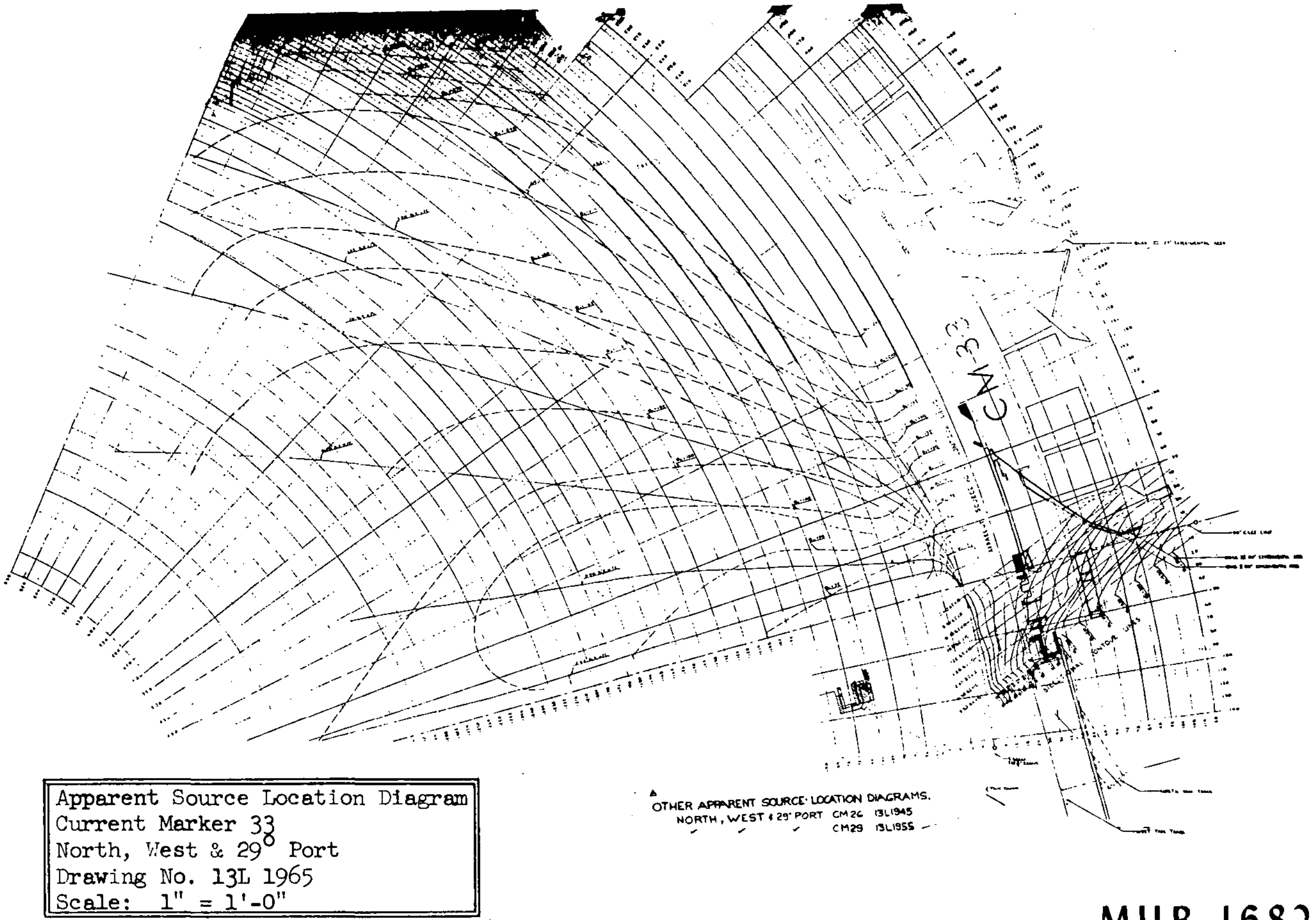

MUB-1682

Fig. 3. Reduced version of Bevatron map showing Source Point and Direction Contours at CM 33 (Dwg. No. 13L1965A).

(ρ_D, θ_D) gives the exit path of the beam in the "field free" region outside the Bevatron.

Example (1): Take as in (a): $p = 0.7$ BeV/c;
Target coordinates: $\rho = 0$ in., $\theta_t = -105$ mrad;
$\rho_s = -26$ in., $\theta_s = -83$ mrad (at CM 26)
$\rho_D = +39$ in., $\theta_D = +9$ mrad.

By joining these two points, the exit path is obtained. From Fig. 1 it can be determined that in this example the beam will not emerge in a useful region, but will strike the steel vacuum-tank support.

Example (2): Target position: $\rho = 0$ in., $\theta_t = -45$ mrad;
$p = 0.7$ BeV/c (at CM 26);
$\rho_s = -5$ in., $\theta_s = -37$ mrad;
$\rho_D = +9$ in., $\theta_D = +22$ mrad.

By joining these points one finds that the 0.7-BeV/c beam from this new target position emerges through the thin external beam window in the west tangent tank, or through the snout in the north tangent tank.

(c) Given a point on the emergent beam (e. g., turning point in first magnet, center of snout or window, etc.), to find the target position.

Lay a straightedge to pass through the chosen point, and note the values of $\theta_D(p)$ and $\theta_s(p)$ where the straightedge intersects the appropriate p-contour lines on the Direction Contour and Source Contour plots. In general, these values are not equal. Rotate the straightedge about the fixed point until the position is achieved where $\theta_D(p) = \theta_s(p)$. This line gives the direction of exit of the beam, and the location θ_t of the target.

B. Comments

(1) Targets. All targets are assumed to be placed at $R_0 = 559\text{-}3/8$ in, the nominal beam centerline.

(2) Interpolation. If interpolation is required, the behavior of the neighboring contour lines should be examined to see how nonlinear the interpolation is likely to be. (Note that the intervals between contour lines are not constant.)

(3) Unobstructed exit of beams. The line joining the points $(\rho_s\ \theta_s)$ and $(\rho_D\ \theta_D)$ determines the path of the beam in the "field-free region" outside the Bevatron. It is quite possible for this straight line to intersect some obstruction, while the beam path—being curved within, and close to the magnet–

could avoid the interference, or vice versa. This is especially true for orbits that emerge where the leg yokes are cut back. In all but marginal cases, it is easy to estimate from the actual target location and the emergent direction whether the beam will indeed clear the interferences.

(4) Contour-plot uses. The most obvious use of the contour plots is to determine the location of a target such that a beam of chosen momentum will emerge through a thin window and enter a quadrupole lens or steering magnet suitably located. Other desirable information which can readily be abstracted includes

(a) The motion of the apparent source as the Bevatron field increases from CM 26 through CM 33.

(b) The change in apparent target size for different points of production, and for different momenta within the momentum bite.

(c) The maximum and minimum momenta obtainable from the same target, i.e., dispersion.

II. MAP CONSTRUCTION

A. Solution of the Orbit Equation

The equation of motion of a charged particle in a magnetic field is

$$\vec{F} = \frac{d\vec{p}}{dt} = \frac{e}{c} (\vec{v} \times \vec{B}) . \tag{1}$$

Using the coordinate system described in Sec. I, we take $B_r = B_\theta = 0$ and $B_z \neq 0$ in the median plane, whereupon Eq. (1) reduces to

$$R'' = R\,\theta' (\beta + \theta'), \tag{2a}$$

and

$$\theta'' = (-R'/R)\,(\beta + 2\theta'), \tag{2b}$$

where $R = r/R_0$, $\beta = B_z/B_0$, $R_0 = 599\text{-}3/8$ in., and B_0 = Normalizing constant (different at each current marker). The prime denotes differentiation with respect to $T = (eB_0/m\gamma c)t$, where t is in seconds. Values of $\beta(r, \theta)$ at CM 26, 29, and 33 have been measured by the Magnet Testing Group.[1] The LRL IBM-650 program ETHELBERT, written by Victor Brady, uses these values of $\beta(r, \theta)$ in the solution of Eqs. (2a) and (2b). The input data needed to trace an orbit are: target position $(\rho_t\, \theta_t)$, particle momentum (p), and angle of production (λ). An estimate of the apparent source can be found by (a) tracing out orbits from an actual target to the "field-free region" outside the Bevatron (Fig. 4) for two values of λ close to the forward direction; then (b) extending tangent lines back from these two orbits to a point of intersection; viz., the apparent source point.

If (r_1 θ_1) and (r_2 θ_2) are points on the trajectories in the field-free region, and the respective production angles are λ_1 and λ_2, then the apparent source coordinates are given by

$$\tan\theta_s = \frac{g_1 - g_2}{g_2 h_1 - g_1 h_2}, \tag{3a}$$

and

$$r_s = \frac{g_1}{\cos\theta_s + h_1 \sin\theta_s}, \tag{3b}$$

where

$$g_i = \frac{r_i}{\cos\theta_i\,(1 + \tan\lambda_i \tan\theta_i)}, \qquad \text{for } i = 1, 2$$

and

$$h_i = \tan(\theta_i - \lambda_i), \qquad \text{for } i = 1, 2 .$$

In constructing the contour plots source points were found in all cases by setting λ_2 = 0 deg and using a variety of values of λ_1 (up to 8 deg) as described in Sec. C.[2]

B. Comments

The qualitative behavior of the contours for θ_t = const can be seen from Fig. 5. The locus of the apparent source for particles crossing an infinite downstream magnet boundary (θ = const) is a smooth curve, concave downward. On the other hand, for particles that cross an infinite orthogonal boundary (r = const), the locus follows a different curve, concave left. In the case of the Bevatron magnet, where both boundaries occur, the locus will be a composite of the two curves, with a transition region corresponding to particles emerging near the corner of the magnetic field. No cusp occurs, of course, since the boundaries are not infinitely sharp.

We found that in all cases the orbits had become essentially straight lines for either $r > R_0 + 60$ in. or $\theta > +50$ mrad, and these conditions were

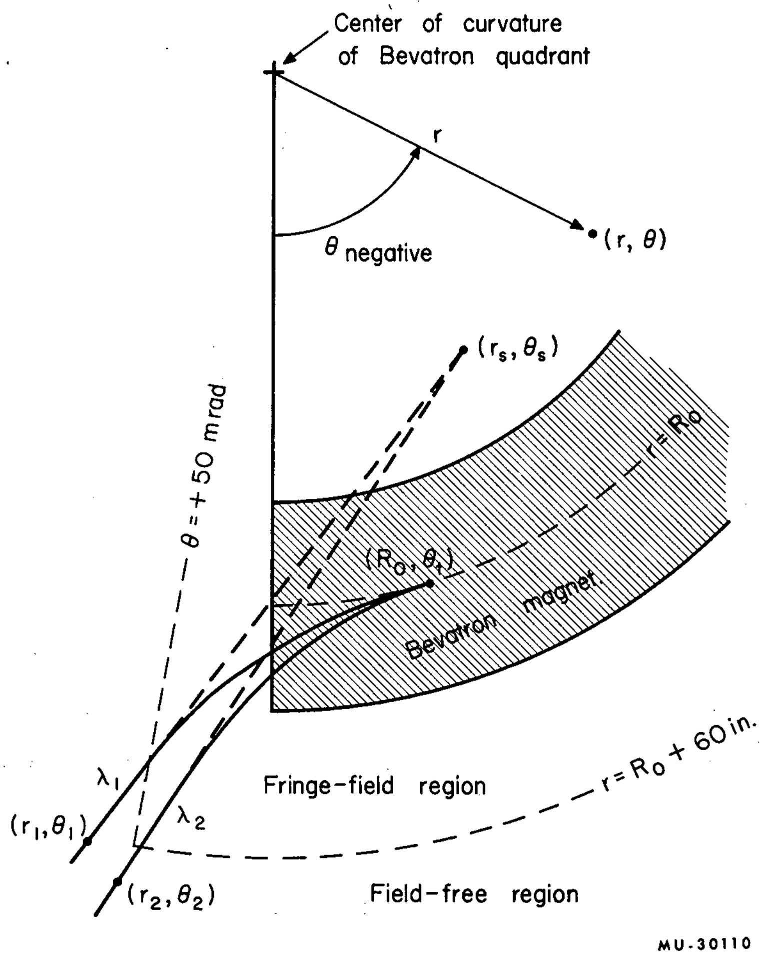

Fig. 4. This shows the definition of the coordinate system (r, θ), the defining boundaries of the "field-free regions," and the method of obtaining the apparent source (r_s, θ_s) from two orbits traced out from a target point (r_t, θ_t). The production angle λ_2 was always taken to be 0 deg.

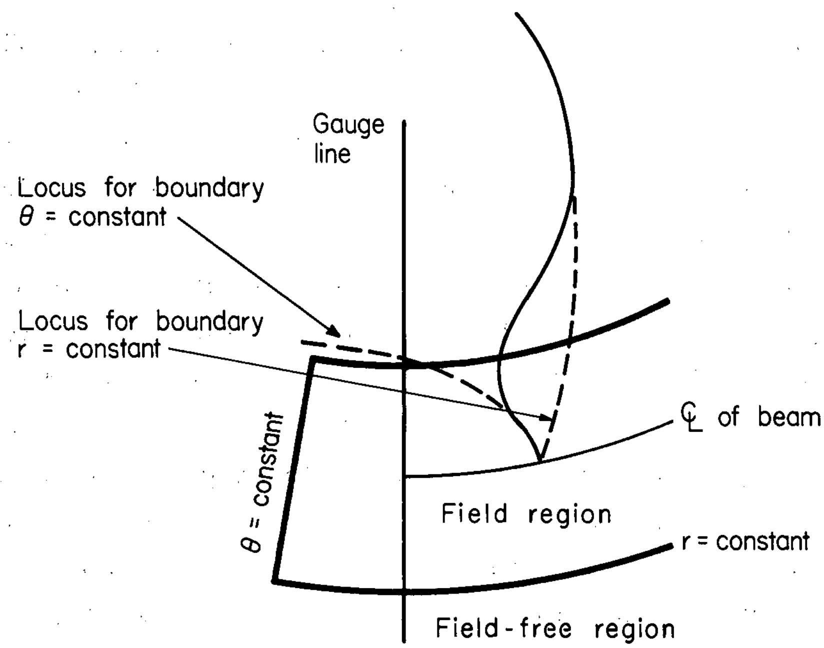

Fig. 5. Qualitative illustration of composition of the θ_t contour line from two loci corresponding respectively to emergence of the beam through end or side of the magnetic field.

applied to halt the calculations in the ETHELBERT program. This orbital property constitutes the definition of the "field-free" region.

III. ERRORS IN SOURCE LOCATION

We define an estimate of a source point as being the intersection of (a) the $\lambda_a = 0$ deg trajectory, with (b) another trajectory having $\lambda_b = \lambda_1$ (± 0 deg). Two estimates based on ($\lambda_b = +\lambda_1$ deg) and ($\lambda_b = -\lambda_1$ deg) respectively, always gave different approximations of the source point, because of aberrations in the effective fringing field "lens." When λ_b was chosen to be large, the discrepancy was also large; if, however, it was taken to be small, then round-off errors in the computer computation produced an unsystematic "jitter" in the estimates. The procedure adopted was to start with some large value for λ_b (e.g., 8 deg), to find the estimates for $\pm\lambda_b$, and then to repeat the computation for successively smaller choices of λ_b ($\lambda_b = 4$ deg, 2 deg, 1 deg, 0.5 deg) until the limit of convergence set by the computer was reached. This limit was found to be $\lambda_b = 2$ deg in most cases. It was found that the midpoint between the two estimates $\pm\lambda_b$ did not change very much as λ_b was varied over the whole range. Therefore, the deviation of this midpoint as λ_b was varied was chosen as a measure of the uncertainty in longitudinal location of the source point by this method. For example, wherever the beam could actually emerge, for $|\theta_t| \leqslant 60$ mrad, the error in the longitudinal location of the apparent source turned out to be less than $\pm 1/4$ in. For $|\theta_t| \geqslant 60$ mrad, the uncertainty was best expressed as a percentage of the distance from the apparent source to the stopping point on the computed orbit, viz., $r - R_0 = 60$ in. or $\theta = +50$ mrad, and was less than 1.4% for CM 33, and less than 2.5% for CM 29. For CM 26, when $|\theta_t| < 150$ mrad, the percentage error was less than 2%, and for $|\theta_t| \geqslant 150$ mrad, it was less than 5%.

IV. MAGNIFICATION

The magnification is defined as $M = \Delta\lambda/\Delta\lambda'$, where $\Delta\lambda$ equals the difference in emission angle of two rays as they leave the target, and $\Delta\lambda'$ equals the difference in direction of the two rays where they are essentially in the Bevatron field-free region. For all particle beams exiting from the snout of the north tangent tank, or the window of the west tangent tank, the magnification varies between 0.90 and 1.00 for CM 26, 29, and 33. For beams that exit from the windows at the ends of Quadrants II and III, the magnification is large and typically lies between 5 and 30. These magnifications were calculated for two rays near zero production angle. Magnification maps, giving the magnification for a particular target position, current marker, and momentum, have been constructed and are available on request.

REFERENCES

1. Peter G. Watson, Engineering Notes Job No. 4901-01, File Nos. M-1 and M-3, August 12, 1955.
2. An addition to the ETHELBERT program called FOCUS (written by V. Brady) was used to solve Eqs. 3a and 3b.